

# STRONG FOCUSING WIGGLER FOR SASE AND FEL IN THE FAR- INFRARED REGION AT ISIR, OSAKA UNIVERSITY

S. Kashiwagi<sup>#</sup>, T. Noda, R. Kato, G. Isoyama,

Institute of Scientific and Industrial Research, Osaka University, Ibaraki, Osaka 567-0047, Japan

S. Yamamoto, K. Tsuchiya,

Institute of Materials Structure Science, KEK, Tsukuba, Ibaraki 305-0801, Japan

## Abstract

We have fabricated an edge-focusing wiggler for FEL and SASE in the far-infrared region at the Institute of Scientific and Industrial Research (ISIR), Osaka University. We have adopted the strong focusing scheme for the wiggler in order to keep the beam size small along the wiggler. The period length of the wiggler is 60 mm, the number of periods is 32, and the total length is 1.938 m, including end magnet blocks for the orbit compensation. The wiggler consists of four FODO cells for double focusing. Focusing elements and defocusing elements are incorporated with single wiggler periods with edge angles of  $+5^\circ$  and  $-5^\circ$ , respectively, and they are separated by 3 normal wiggler periods. In this paper, we report fabrication of the strong focusing wiggler and results of the magnetic field measurement.

## INTRODUCTION

We have proposed a novel wiggler, named the edge-focusing (EF) wiggler, which produces the strong transverse focusing field incorporated with the normal wiggler field [1]. The first model of the EF wiggler has been fabricated to demonstrate its principle and to evaluate its performance. It is a five-period planar wiggler with an edge angle of  $2^\circ$  and a period length of 60 mm. It is experimentally confirmed that a field gradient of 1.0 T/m is realized along the beam axis in the EF wiggler [2,3].

As a next step, we apply the EF scheme to the wiggler being used for FEL and SASE in the far-infrared region at the Institute of Scientific and Industrial Research (ISIR), Osaka University to make the gain length of SASE shorter by keeping the beam size small along whole the wiggler. The wiggler is a conventional Halbach-type wiggler and we replace only its magnet parts with new ones. We, therefore, hold the wiggler parameters same as before: the period length is 60 mm and the number of periods is 32. As the electron beam energy of 10-30 MeV is relatively low and the magnetic field of the wiggler up to 0.4 T at the minimum wiggler gap of 30 mm is high in our experimental conditions, the natural focusing force in vertical direction is strong in the wiggler and it is strongly dependent on the electron energy and the magnet gap of the wiggler. The focusing forces should be comparable to or higher than the strong natural focusing force, equally in the horizontal and vertical directions over the wide range of the electron beam energy and the wiggler gap. In order

<sup>#</sup>shigeruk@sanken.osaka-u.ac.jp

to meet this requirement, we adopt the strong focusing scheme using the EF wiggler. Focusing and defocusing elements are composed of permanent magnet blocks with the edge angle and they are alternately inserted in magnet arrays of the wiggler. The strong focusing wiggler has been fabricated and the magnetic field has been measured at KEK.

## STRONG FOCUSING WIGGLER

The edge-focusing wiggler is basically a Halbach type wiggler made only of permanent magnet blocks, but their shapes are not rectangular parallelepipeds. The average focusing force of the EF wiggler can be calculated using the simple model of the wiggler composed of alternating bending magnets with the edge angle. The field gradient is approximately proportional to the edge angle  $\phi$  and hence the focusing force along the wiggler can be easily adjusted with the edge angle. The focusing force of the EF wiggler of the horizontal oscillation type is  $k_x = 1/B\rho(dB_y/dx)$  in horizontal direction and  $k_y = k_0 - k_x$  in the vertical direction, where  $k_0$  is the natural focusing force of the wiggler in the vertical direction and  $k_0 = k_x + k_y$ .

In the first model of the EF wiggler, the edge angle was  $2^\circ$  and the weak focusing scheme was adopted, to focus an 11.5 MeV electron beam both in the vertical and horizontal directions equally and simultaneously at the minimum wiggler gap of 30 mm, by making use of the strong natural focusing force in the vertical direction. All the permanent magnet blocks have the same edge angle and the field gradient is produced along the whole wiggler length. The natural focusing force, however, decreases quickly with increasing the electron energy or the wiggler gap, or both, while the focusing force produced with the edge angle decreases slowly. When the defocusing force produced with the edge angle exceeds the natural focusing force in the vertical direction, the double

Table 1: Main parameters of the SF wiggler

Block sizes	90x20x15 mm <sup>3</sup>
Magnet materials (Coating)	Nd-Fe-B (TiN)
Period length	60 mm
Number of periods	32 periods
Total length	1.938 m
Peak magnetic field	0.39 T (gap 30mm)
Number of FODO cells	4 cells
Length of FODO cell	0.48 m
Edge angle	$\pm 5^\circ$
Field gradient	$\pm 3.2$ T/m

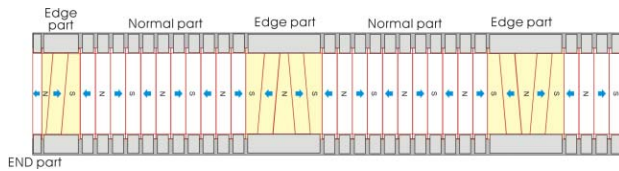


Figure 1: Part of the magnet array of the strong focusing wiggler. Left side is the end part of the wiggler.

focusing condition breaks down. In our experiments of FEL and SASE, the wide range of the electron energy and the wiggler gap is used and hence the double focusing condition does not necessarily fulfilled, so that the weak focusing scheme is not appropriate. We have, therefore, adopted the strong focusing scheme for the new wiggler.

In the strong focusing scheme, the electron beam is focused alternatively in the vertical and the horizontal directions to obtain focusing in the both directions using a sequence of focusing and defocusing elements separated by drift spaces, which is called the FODO lattice. The betatron function in a FODO lattice varies periodically from the minimum value at the defocusing element to the maximum one at the focusing element. When the magnitude of the focusing force, denoted by  $k$ , is equal to that of the defocusing force, the geometric mean of the betatron function is given by  $\bar{\beta} = \sqrt{\beta_F \cdot \beta_D} = 2/k$  in a simple thin lens approximation, where  $\beta_F$  and  $\beta_D$  are betatron functions at focusing and defocusing elements, respectively. The phase advance  $\mu$  is given by  $\sin(\mu/2) = kl/2$ , where  $l$  is the length of a unit cell of the FODO lattice and  $kl$  must be less than 2. To make the betatron function small,  $k$  should be large, but at the same time  $k$  has to be less than  $2/l$ . This means that, if  $\mu$  is fixed at a certain value,  $\bar{\beta}$  is reduced with increasing  $k$ , while  $l$  has to be made short as  $l = 2/k$ . The focusing strength of the edge-focusing wiggler is approximately proportional to the edge angle and can be varied over the wide range, while making the cell length short results in the number of FODO cells increasing, which will eventually reach technical limitations.

In design of the wiggler, we have optimised parameters of the FODO lattice to meet the requirements of our experiment. Fig. 1 shows a part of a magnet array of the strong focusing wiggler (SF wiggler) and the parameters are listed in Table 1. The permanent magnet used is NdFeB (NEOMAX-38VH, NEOMAX Co.) with  $B_r = 1.22$  T and the peak magnetic field of the EF wiggler is 0.39 T at the minimum gap of 30 mm. The number of FODO cells in the wiggler is four and the cell length is 0.48 m. The number of cells is a factor of the number of wiggler periods, 32. Focusing elements are single wiggler periods with the edge angle of  $+5^\circ$  and defocusing ones are those with  $-5^\circ$ , and they are separated by 3 normal wiggler periods. The magnitude of field gradient at focusing and defocusing elements is about 3.2 T/m at the wiggler gap of 30 mm and the phase advance in the FODO lattice is chosen to be approximately 60 degrees for a 10 MeV electron beam. Longitudinally magnetized blocks are added at both ends of the strong wiggler in

order to compensate for the horizontal shift of the oscillatory beam orbit due to the fringing magnetic field at the ends. Thus the total length of the SF wiggler is 1.938 m.

### Fabrication of permanent magnet blocks

Before machining magnetic blocks, we measured the surface magnetic field of one of the raw magnet blocks using a Hall probe to examine homogeneity of magnetization in the material block. From this measurement, it was found the center of the magnetic field distribution was shifted approximately by 2 mm from the mechanical center of the block. The magnet blocks were molded by the vertical press with the magnetic field applied perpendicular to the press direction, or horizontally, and the shift is along the press direction. Since the height of the mold placed in a pair of electromagnet coils is adjusted with spacers, it is thought that the mold was placed 2 mm lower than the central axis of the coils. It is possible to identify the direction of press and the upper and lower sides of the raw magnet blocks by their shape, so that all the magnet blocks were machined with respect to the magnetic center of the raw magnet blocks.

Nine types of permanent magnet blocks, among which two types are for normal wiggler periods, one type for the orbit compensation, and the remaining 6 types for EF wiggler periods, were fabricated with spare blocks 10 % more in number for each type. The magnetic field produced by each magnet block was measured using a Hall probe and a flipping coil. The magnetic field was measured four times for each magnet block with the Hall probe; two measurements with and without rotation by  $180^\circ$  around the magnetization axis on the North-pole side and those on the South-pole side. The standard deviation of the measured magnetic field is approximately 0.2 % for magnet blocks used in normal wiggler periods. The standard deviation of the magnetic field asymmetry between the North pole and the South pole is approximately 0.03 % for the same magnet blocks. We selected the necessary number of magnet blocks to be used for the SF wiggler in view of reducing the standard deviations of the magnetic field and the magnetic field asymmetry.

Each magnet block for the normal wiggler periods and for the orbit compensation at the ends is set in a holder made of the nonmagnetic stainless steel, SUS316, and mechanically clamped, while five magnet blocks, or three at the both ends, for one of two pairs for an EF period, that is, an upper pair and a lower one, are glued each other to a single block and mechanically fixed in a holder. These magnet units are installed on four pairs of base plates made of the stainless steel, SUS 304, and they are installed on the mechanical frame of the wiggler.

### Initial arrangement of wiggler magnets

The initial arrangement of the magnet blocks was determined separately for the normal wiggler periods and the EF periods. A pair for an EF period consists of five

magnet blocks, which are three vertically magnetized blocks with the trapezoid shape and two longitudinally magnetized blocks with the parallelogram shape. The combination of these five magnets is determined in terms of the measured surface magnetic field so that a dispersion of the field strengths became minimum for each unit. The vertical magnetic field integrated along the beam axis ( $B_{VS}$ ) for EF units was measured using a flipping coil. Combinations of two units to make a pair were determined so that a difference in field integrals became minimum for each pair. These pairs were arranged in the ascending order of differences in field integrals from the upstream of the wiggler.

On the other hand, the magnet arrangement in the normal magnet part was determined on the basis of the field integral measured for each magnet block with the flipping coil by means of the simulated annealing algorithm proposed by Cox and Youngman [4]. In this process, we assumed that normal wiggler magnet blocks with the mean strength existed in the EF wiggler periods, as the computer code we used cannot take magnet blocks with different shapes into account and also the measurement of the field integral was not same for all kinds of magnet blocks.

## MAGNETIC FIELD MEASUREMENT

### *Setup for measurement*

The magnetic field of the SF wiggler was measured at the High Energy Accelerator Research Organization (KEK), using a magnetic sensor with two Hole probes for simultaneous measurement of the vertical and the horizontal field components, which is mounted in a small oven to control the temperature of the sensor. The Hole probes were calibrated with a NMR magnetic field sensor. The magnetic sensor was mounted on a 3-axis linear stage, and the magnetic field was measured along the wiggler axis or the z-axis by a 1 mm step at various transverse positions specified by x and y coordinates.

As described previously, the magnet blocks for the SF wiggler are mounted on four pairs of base plates, which will be installed on the mechanical frame at ISIR, Osaka University in place of the present magnet blocks. For the magnetic field measurement, we use the mechanical frame of an in-vacuum undulator being developed at KEK. The SF wiggler mounted on four pairs of base plates were installed on the mechanical frame of the KEK undulator using attachments made of steel, so that the wiggler gap can be changed in the magnetic field measurement. The magnetic field measurement system was aligned in parallel with the SF wiggler using a standard ceramic block and a theodolite, and the original position of the coordinate system for the measurement was determined vertically by the symmetry point of the vertical magnetic field and longitudinally by several peak positions of the vertical magnetic field.

### *Optimization of the magnetic field*

We corrected the magnetic field of the wiggler by inserting small magnet chips into holes drilled in magnet holders and by exchanging some magnet blocks. In the correction process, the magnetic field was, firstly, measured along the wiggler axis using the Hall probe at the 30 mm wiggler gap. Then the first and the second integrals were calculated with the measured magnetic field. The first field integral over a half wiggler period corresponding to the n-th magnet pole defines the deflection of the electron beam caused by the  $n$ th magnet pole and it is given by

$$I_{1n} = \int_{z_n}^{z_{n+1}} B_y(z) dz,$$

where  $z_n = n\lambda_w/2$  is  $B(z)$  are the boundary between the n-th and (n-1)-th poles and  $B_y(z)$  is the vertical magnetic field as a function of z. The deviation of  $I_{1n}$  is defined as

$$i_n = (|I_{1n}| - \langle I \rangle) / \langle I \rangle,$$

where  $\langle I \rangle$  is the mean value of  $|I_{1n}|$  [5]. The second field integral at the longitudinal position in the wiggler is given by

$$I_2(z) = \int^z \int^{z'} B_y(z'') dz'' dz'.$$

The second integral is proportional to the electron trajectory in the wiggler. The first and second integrals were used to find problematic magnet blocks and the magnet field was corrected mainly by exchanging magnet blocks. For magnetic field correction at EF wiggler periods, some pairs of the units were slightly shifted in the horizontal direction to adjust the field integral. The electron trajectory was less deflected horizontally at the entrance and the exit of the SF wiggler due to insufficient kicks made with the first and the last half poles. They are one of the magnet blocks for a half EF wiggler period and the magnetic field was adjusted by adding permanent magnet tips in the folders.

### *Results of the field measurement*

After completing these magnetic adjustments, we measured the magnetic field of the SF wiggler at various transverse positions along the wiggler axis at several magnet gaps ranging from 30 to 50 mm, and derived electron trajectories and field gradients using the measured magnetic field. Figure 2 shows the vertical magnetic field distribution along the wiggler at a magnet gap of 30mm. The peak wiggler field is approximately 0.392 T. The measured field distribution is in good agreement with calculation one using the magnetic charge method [6]. The maximum deviation of the measured field from the calculated one is 13 mT for the peak magnetic field of 0.392 T, which occurs at a position where the magnetic field is close to zero. Figure 3 shows electron trajectories in the SF wiggler calculated for 11 MeV energy with the measured magnetic field at 30 mm and 40 mm wiggler gaps. The solid and the dashed lines show horizontal and vertical trajectories, respectively. In the case of the 40 mm wiggler gap in Fig. 3, the electron

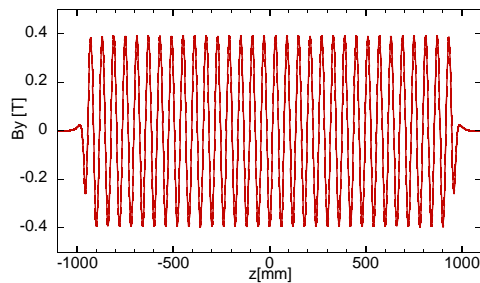


Figure 2: Measured vertical magnetic field ( $B_y$ ) along the longitudinal axis at gap = 30 mm.

beam are assumed to enter into the SF wiggler with small angles both in the horizontal and the vertical directions, in order to make the orbit displacements at the exit small. The distortions of the electron trajectories are considerably smaller than the oscillation amplitudes of the wiggler in the both cases. Except for amplitudes of the oscillation, the calculated electron beam orbits are hardly changed at the two wiggler gaps, indicating that the SF wiggler works as a wiggler at different gaps and its magnetic field is as good as that of a normal wiggler.

The horizontal and the vertical field gradients ( $dB_y/dx$  and  $dB_x/dy$ ) of the SF wiggler are derived from the magnetic field measured along the longitudinal axis at several horizontal and vertical positions on each axis. Figure 4 shows the horizontal and the vertical field gradients derived by the linear fitting of measured values of the magnetic field at the wiggler gap of 30 mm. The high field gradient is generated in both the horizontal and the vertical directions. The peak field gradient is approximately 3.2 T/m at the 30 mm wiggler gap, which is produced with the EF wiggler periods with the edge angle of  $+5^\circ$  or  $-5^\circ$ . The field gradient integrated over a single EF period is calculated for seven EF wiggler periods both in the horizontal direction and the vertical one. The seven values for the horizontal direction agree quite well with each other with errors of approximately 1 %, and so does for the vertical direction, but the mean value of the integrated field gradient for the vertical

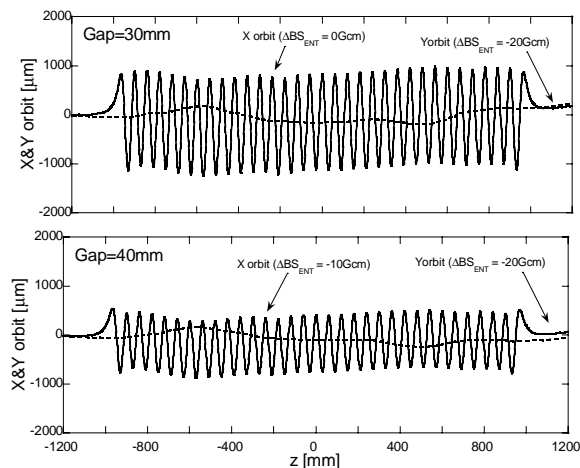


Figure 3: Horizontal and the vertical electron trajectories calculated with the measured magnetic field at 30 mm and 40 mm gaps. The electron beam energy is assumed to be 11 MeV.

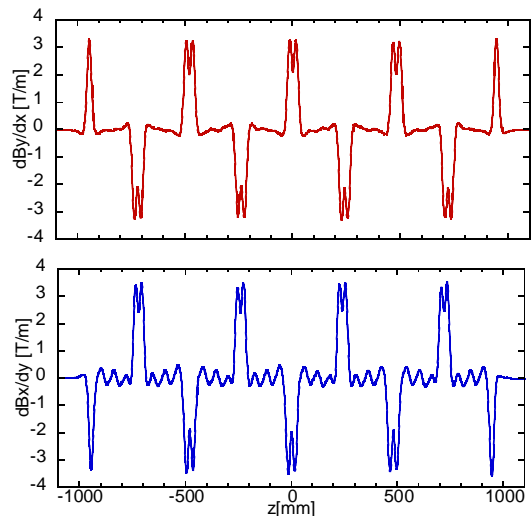


Figure 4: Horizontal (upper) and the vertical (lower) field gradients ( $dB_y/dx$ ,  $dB_x/dy$ ) derived with the measured magnetic field at gap = 30 mm.

direction is larger than that for the horizontal direction by approximately 5 %, the reason of which is not yet known. There might be some problems in the measurement of the vertical magnetic field for deriving the field gradient, since the base line of the vertical field gradient shown in Fig. 4 oscillates periodically in the regions where no field gradient is expected. On the other hand, the mean value of the field gradient in the horizontal direction agrees well with the calculated value with an error of approximately 1 %.

### Acknowledgements

The authors would like to thank Messrs. S. Okada, T. Kohda, K. Okihira, M. Yuki and T. Iwamoto of NEOMAX Co., Ltd. for their help on the fabrication and the magnetic field measurement of the SF wiggler. This research was partly supported by the Joint Development Research at the High Energy Accelerator Research Organization (KEK), 2005-18, 2005 and The Ministry of Education, Culture, Sports, Science and Technology (MEXT), Grant-in-Aid for Exploratory Research, 15654036, 2003&2004 and for Young Scientists (B), 17740144, 2005.

### REFERENCES

- [1] G. Isoyama et al., Nucl. Instr. and Meth. A 507 (2003) 234
- [2] S. Kashiwagi et al., Nucl. Instr. and Meth. A 528 (2004) 203
- [3] S. Kashiwagi et al., Proceedings of FEL 2004 Conference, p458, 2004
- [4] A. D. Cox and B. P. Youngman, SPIE 582, 91 (1985).
- [5] T. Tanaka et al., Nucl. Instr. and Meth. A 465 (2001) 600-605
- [6] G. Isoyama, Rev. Sci. Instrum., Vol. 60, No. 7 (1989) 1826